Laser-Light-Scattering Studies on the Complexation between Poly(styrene-*co*-4-vinylphenol) and Isorefractive Poly(ethyl methacrylate) in Toluene

Yubao Zhang,[†] Maoliang Xiang,[‡] Ming Jiang,[‡] and Chi Wu*[,†]

Department of Chemistry, The Chinese University of Hong Kong, Shatin, Hong Kong, and Institute of Macromolecular Science, Fudan University, Shanghai 200433, China

Received August 8, 1996; Revised Manuscript Received December 2, 1996[⊗]

ABSTRACT: Laser-light-scattering (LLS) studies on the complexation between poly(styrene-*co*-4-vinylphenol) (STVPh) and isorefractive poly(ethyl methacrylate) (PEMA) in toluene show that the complexes can form immediately after mixing two complementary polymer solutions. The time dependence of the excess scattering intensity and average hydrodynamic radius ($\langle R_h \rangle$) indicates that the STVPh/PEMA complex dispersion is not thermodynamically stable in toluene. Only if one of the components is in excess can more stable complex dispersion be obtained. When the phenol content of STVPh is higher than 9 mol %, the composition dependence of $\langle R_h \rangle$ shows a maximum at an equimolar ratio of monomer STVPh to EMA, corresponding to the fixed mean stoichiometry (FMS) ratio of complexation determined by viscometry. A combination of static and dynamic LLS results reveals that the complex particles are more compact than individual polymer chains and the complexes have a fixed composition when the amount of STVPh15 is in excess, wherein each PEMA polymer chain acts as a nucleus surrounded by ∼35 STVPh15 polymer chains, suggesting a sterically controlled complexation process.

Introduction

The miscibility between different polymers is one of the basic factors governing the morphologies and properties of polymer blends. The general method of enhancing the miscibility is to introduce specific interactions,[1] such as ion−ion,[2] electron transfer,[3] and hydrogen bonding.[4−9] Kwei and co-workers[9] first introduced hydrogen-bonding interaction to improve the miscibility of a polymer blend. Coleman *et al.*[8] have developed a semiquantitative theory which predicts the phase diagram (miscibility) of a polymer blend. Jiang *et al.*[5] synthesized a copolymer of styrene and the hydroxyl-containing monomer *p*-(1,1,1,3,3,3-hexafluoro-2-hydroxypropyl)-α-methylstyrene [denoted as PS(OH)] and studied its miscibility with poly(methyl methacrylate) (PMMA). It was found that only ∼2 mol % of the hydroxyl-containing units in PS(OH) rendered the otherwise immiscible blend miscible. When the interaction increases, the polymer chains can even form intermolecular complexes.[10,11] The immiscibility-to-miscibility and miscibility-to-complexation transitions can be induced by the same kind of intermolecular interaction, but the difference is that the complexation involves pairing of the interacting polymer chains, whereas in a normal miscible blend different component chains are believed to be randomly mixed. Therefore, the study of the complexation between two polymer chains with a specific interaction has opened a new way to develop new materials from existing common polymers.

Intermolecular complexation has been extensively studied.[12−14] According to the type of interaction, the complexation can be divided into four classes: (1) polyelectrolyte complexation; (2) hydrogen-bonding complexation; (3) stereocomplexation; and (4) charge-transfer complexation. The polyelectrolyte and hydrogen-bonding complexation have been mostly studied. Most of the studies in the past are concentrated on the complexation of water-soluble polymers in aqueous solution or in a strong polar solvent. Little was reported on the complexation of lipophilic polymers, especially those large-scale commercial products with a wide range of applications. Frechet and de Meftahi[15] and Goh *et al.*[16] reported the complexation between poly(vinylphenol) (PVPh) and poly(vinylpyridine). The DSC results showed that this kind of polymer blend has a much higher T_g than the individual components, indicating a strong interaction between the two components. Goh *et al.*[17] have also studied the miscibility and complexation between poly(styrene-*co*-allyl alcohol) (PSAA) and poly(*N*,*N*-dimethylacrylamide) (PDMA) in butanone. Kwei *et al.*[18] found complexation between PVPh and PDMA in dioxane and methanol. Jiang *et al.*[10,11] have found that PMMA can form complexes with PS(OH) in both toluene and bulk if the hydroxyl content of PS(OH) is higher than ∼7 mol %. Since then, this system has been extensively studied using various methods, such as viscometry, fluorospectroscopy, and high-resolution NMR. The advantage of studying this system is that the interaction strength can be well controlled by varying the hydroxyl content so that the same blend system can transfer from immiscibility to miscibility and from miscibility to complexation.

Spectroscopy methods, such as UV, IR, fluorescence, and especially NMR, are powerful methods in elucidating the formation and the local structure of the complexes in solution. On the other hand, laser light scattering (LLS) has proved to be a very useful method to study the aggregation process, especially in a very dilute solution wherein conventional viscometry has no sensitivity. In this study, the formation and the structure of the complex between poly(styrene-*co*-4-vinylphenol) (STVPh) and poly(ethyl methacrylate) (PEMA) in toluene have been studied by a combination of static and dynamic LLS. In this system, toluene is inert to the hydrogen bonding and is isorefractive to PEMA. This study was motivated with three objectives: (1) to find direct evidence of the complexation between STVPh

* To whom correspondence should be addressed.
† The Chinese University of Hong Kong.
‡ Fudan University.
⊗ Abstract published in *Advance ACS Abstracts,* March 1, 1997.

S0024-9297(96)01190-4 CCC: $14.00

Table 1. LLS Results of Individual Poly(styrene-*co*-4-vinylphenol) and Poly(ethyl methacrylate) Chains in Toluene or THF at 25 °C

sample	phenol, mol %	M_w, 10^5 g/mol	A^2, 10^{-4} mL mol/g^2	$\langle R_g \rangle$, nm	$\langle R_h \rangle$, nm	$\langle R_g \rangle / \langle R_h \rangle$
STVPh0[a]	0	3.1				
STVPh3	3	1.0	4.9	12	9	1.4
STVPh6	6	3.7	1.0	40	26	1.5
STVPh9	9	4.0	3.4	43	27	1.6
STVPh12	12	3.9	1.3	39	26	1.5
STVP15	15	3.9	0.6	35	23	1.5
PEMA-1[b]		8.0	3.6	64	40	1.6
PEMA-2[a]		0.7				

[a] Characterized by GPC. [b] In THF.

and PEMA in very dilute solution; (2) to reveal the composition and interaction dependence of the complexation; and (3) to elucidate the mechanism of the interaction and the resulting structure of the complexes.

Experimental Section

Sample Preparation. Poly(ethyl methacrylate) (PEMA) was synthesized by radical polymerization of ethyl methacrylate in benzene.[7] Poly(styrene-*co*-4-vinylphenol)s (STVPh) with different contents of 4-vinylphenol (VPh) were prepared by copolymerization of styrene and 4-methoxystyrene followed by a demethylation procedure.[19] The weight-average molar masses of PEMA and STVPh listed in Table 1 were determined by laser light scattering. In Table 1, the number following STVPh represents the molar percent of VPh content in the copolymer. There is no detectable aggregation if the toluene solution contains only STVPh.

All solutions used in laser light scattering were clarified with a 0.2-μm Whatman PTFE filter. The solution mixture was prepared by adding dropwise a proper amount of a dust-free PEMA solution to ~1 mL of dust-free STVPh solution. The weight of 1 drop of the solution is ~0.01 g, and the adding rate is about 1 drop/s. The solution was vigorously mixed using a Vortex mixer. The measurement time started just after the addition. The initial concentrations of both the STVPh and the PEMA solutions were 1.00×10^{-4} g/mL except where otherwise specified. The final composition of each mixture was determined by weighting.

Laser Light Scattering. A modified commercial LLS spectrometer (ALV/SP-125) equipped with a multi-τ digital time correlator (ALV-5000) and a solid-state laser (ADLAS DPY 425 II, output power ≅ 400 mW at $\lambda_0 = 532$ nm) was used. The incident beam was vertically polarized with respect to the scattering plane. All measurements were done at 25.0 ± 0.1 °C. The specific refractive index increment (dn/dC or written as ν) was determined by a novel and precise differential refractometer.[20] For STVPh with different VPh contents, ν ranges from 0.110 to 0.115 mL/g, while for PEMA ν is only ~0.006 mL/g. Therefore, the light scattered from PEMA can be neglected in comparison with that from STVPh.

In static LLS, the angular dependence of the excess absolute time-averaged scattered intensity, known as the Rayleigh ratio $R_{vv}(q)$, of a set of dilute copolymer solutions was measured. $R_{vv}(q)$ is related to the weight-average molar mass M_w, the second virial coefficient A_2, and the z-average radius of gyration $\langle R_g^2 \rangle_z^{1/2}$ (or written as $\langle R_g \rangle$) as[21]

$$\frac{KC}{R_{vv}(q)} \cong \frac{1}{M_w}\left(1 + \frac{1}{3}\langle R_g^2 \rangle_z q^2\right) + 2A_2C \qquad (1)$$

where $K = 4\pi^2 n^2 \nu^2/(N_A \lambda_0^4)$ with N_A, n, and λ_0 being Avogadro's constant, the solvent refractive index, and the wavelength of light in the vacuum, respectively. $q = (4\pi n/\lambda_0)\sin(\theta/2)$, with θ being the scattering angle. The copolymer concentration is in units of grams/milliliter.

It should be noted that eq 1 is only valid for homopolymers. When using it for a copolymer, the measured M_w is an apparent one, i.e., $M_{w,app}$. In this study, the ν values of the styrene and VPh segments are not very different. For example, the value of ν for poly(4-methoxystyrene) in toluene is 0.101 mL/g at 25 °C and $\lambda = 546$ nm,[22] only ~10% less than that of polystyrene homopolymer. It is known that for a copolymer with polydispersity in both the chain length and composition, the measured apparent molecular weight M_{app} can be expressed as $M_{app} = (1/\nu^2)\sum_i \Omega_i M_i \nu_i^2$, with ν and ν_i being the specific refractive index increments of the copolymer and the ith polymer chain, respectively, and W_i and M_i being the weight fraction and molar mass of the ith polymer chain, respectively. If the ith polymer chain is comprised of segments A and B with weight fractions of W_{iA} and W_{iB} and refractive index increments of ν_A and ν_B, respectively,[23]

$$M_{app} = \sum_i W_i M_i \left[\frac{W_{iA}\nu_A + W_{iB}\nu_B}{\nu}\right]^2 =$$

$$M_w + 2\sum_i W_i M_i \delta W_{iA}\left(\frac{\nu_A - \nu_B}{\nu}\right) + \sum_i W_i M_i (\delta W_{iA})^2 \left(\frac{\nu_A - \nu_B}{\nu}\right)^2 \qquad (2)$$

where δW_{iA} is the fluctuation of the weight fraction of component A in the ith polymer chain. In this study, the difference in ν between the styrene and VPh segments should be no more than 0.01 mL/g and the component fluctuation is less than 30% because the maximum amount of VPh in the STVPh samples used is ~15 wt %. Therefore, the error of M_w should be less than 6%; namely, $|M_{app} - M_w|/M_w \approx 2 \times 0.3 \times 0.01/0.1 + 2 \times 0.3^2 \times (0.01/0.1)^2 \approx 6\%$. In the complex dispersion, we used the value of ν of the STVPh copolymers in the calculation because PEMA is isorefractive. Thus, the calculated M_w only contains the contributions from STVPh. Assuming f is the weight fraction of the STVPh polymer chains in the complex, we have $\nu_{complex} = \nu_{STVPh} f$, $C_{complex} = C_{STVPh}/f$, and $M_{complex} = M_{STVPh}/f$ so that $[K_{STVPh} C_{STVPh}/R_{vv}(q)]_{C\to 0, q\to 0} = 1/M_{STVPh}$, where K_{STVPh} is the optical constant using the value of ν of the STVPh copolymers. In this study, the weight fraction of PEMA in the complex is less than 15% and $\nu_{PEMA} = 0.006$ mL/g so that the errors introduced into ν and M_w are no more than ~1% and ~2%, respectively, if ν_{STVPh}, instead of ν, is used, well within our experimental error limits.

In dynamic LLS, the intensity−intensity time correlation function $G^{(2)}(t,q)$ in the self-beating mode was measured. $G^{(2)}(t,q)$ can be related to the normalized first-order electric field time correlation function $|g^{(1)}(t,q)|$ as [24,25]

$$G^{(2)}(t,q) = \langle I(0,q)\, I(t,q)\rangle = A[1 + \beta |g^{(1)}(t,q)|^2] \qquad (3)$$

where A is the measured baseline, β is a parameter depending on the coherence of the detection, and t is the delay time. For a polydisperse sample, $|g^{(1)}(t,q)|$ is related to the line-width distribution $G(\Gamma)$ as

$$|g^{(1)}(t,q)| = \langle E(0,q)\, E^*(t,q)\rangle = \int_0^\infty G(\Gamma) e^{-\Gamma t}\, d\Gamma \qquad (4)$$

$G(\Gamma)$ can be calculated from the Laplace inversion of $G^{(2)}(t,q)$ on the basis of eqs 3 and 4. In this study, the constrained regularization CONTIN program developed by Provencher[26] was used. For a diffusive relaxation, Γ is a function of both C and q; namely,[27, 28]

$$\Gamma/q^2 = D(1 + k_d C)(1 + f\langle R_g^2 \rangle_z q^2) \qquad (5)$$

where D is the translational diffusion coefficient at $C \to 0$, and $q \to 0$; f is a dimensionless constant, and k_d is the diffusion second virial coefficient. D, f, and k_d can be obtained from $(\Gamma/q^2)_{C\to 0, q\to 0}$, $(\Gamma/q^2)_{C\to 0}$ vs q^2, and $(\Gamma/q^2)_{q\to 0}$ vs C, respectively. Further, D can be converted to the hydrodynamic radius (R_h) using the Stokes−Einstein equation: $R_h = k_B T/6\pi\eta D$, where η is the solvent viscosity, k_B is the Boltzmann constant, and T is the absolute temperature.

Results and Discussion

1. Time Dependence of Complexation. Upon the addition of PEMA into a STVPh toluene solution, the

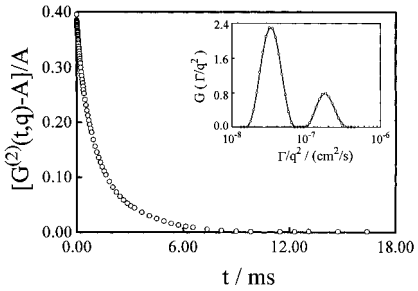

Figure 1. Typical normalized intensity−intensity time correlation function $[g^{(2)}(t,q) - A]/A$ of the STVPh9/EMA-2 solution blend 10 h after preparation. The insert shows an apparent translational diffusion coefficient distribution $G(\Gamma/q^2)$ calculated from the Laplace inversion of $[g^{(2)}(t,q) - A]/A$.

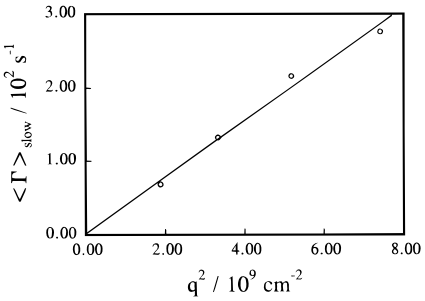

Figure 2. Typical q^2 dependence of the average line width $\langle\Gamma\rangle$ of the slow relaxation process shown in the insert of Figure 1.

scattering intensity gradually increases and so does the measured apparent hydrodynamic radius. The rate increases with the phenol content. Figure 1 shows a normalized intensity−intensity time correlation function $[g^{(2)}(t,q) - A]/A$ for a STVPh9/PEMA-2 solution mixture 10 h after the preparation. The insert in Figure 1 shows an apparent translational diffusion coefficient distribution $G(\Gamma/q^2)$ calculated from the Laplace inversion of $[g^{(2)}(t,q) - A]/A$ on the basis of eqs 3 and 4. $G(\Gamma/q^2)$ shows two distinct relaxation processes. Due to the isorefractive index of PEMA-2 in toluene, what we "see" in LLS is only the contribution from STVPh9. The fast relaxation process can be attributed to the translational diffusion of individual STVPh9 chains. Figure 2 shows a typical q^2 dependence of the average line width $\langle\Gamma\rangle_{slow}$ of the slow relaxation process in Figure 1. The linear dependence of $\langle\Gamma\rangle_{slow}$ on q^2 indicates that the slow relaxation is diffusive and related to the translational diffusion of some large species; namely, it reflects the existence of the complexation between STVPh9 and PEMA-2. This complexation has also been observed by nonradiative energy-transfer (NRET) fluorospectroscopy.[29]

Figure 3 shows the evolution of the translational diffusion coefficient distribution $G(D)$ of a STVPh9/PEMA-2 toluene solution after the mixing, where the scattering angle was fixed at 15° and the weight ratio of STVPh9:PEMA-2 is 100:8. The initial broadening of the peaks in $G(D)$ reflects the formation of a small amount of STVPh/PEMA clusters. These STVPh/PEMA clusters gradually combine with each other to form larger STVPh/PEMA clusters. After ∼70 min, two distinct peaks appear in $G(D)$. Peak 1 corresponding to the size of ∼20 nm is clearly related to individual STVPh9 chains, while peak 2 with a large size (150−300 nm) can be attributed to the STVPh/PEMA complexes. Figure 3 shows that the position and area of peak 2 increase and the area of peak 1 decreases as the time increases, but the position of peak 1 remains the same. This shows that individual STVPh9 chains are gradually incorporated into the STVPh/PEMA complexes. It should be noted that dynamic LLS is a very sensitive method to detect the complexation because $G(D)$ is proportional to the scattering intensity, i.e., to the square of the scatter's mass. Therefore, the larger area of peak 2 actually reflects only a small number of STVPh/PEMA complexes. In other words, Figure 3 shows that in solution, a large amount of STVPh9 remains as individual polymer chains.

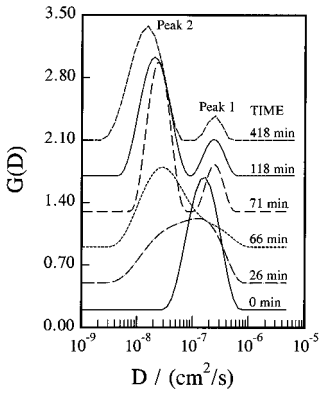

Figure 3. Evolution of the translational diffusion coefficient distribution $G(D)$ of the STVPh9/PEMA-2 solution blend after mixing, where the total polymer concentration is 1.00×10^{-4} g/mL, the weight ratio of STVPh9:PEMA is 100:8, and the scattering angle is 15°.

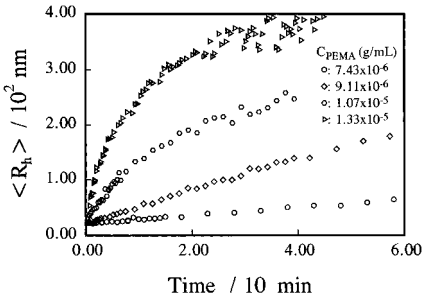

Figure 4. Time-dependence of the apparent hydrodynamic radius of the STVPh9/PEMA-2 solution blend with different compositions, where the STVPh9 concentration is 1.00×10^{-4} g/mL and the scattering angle is 15°.

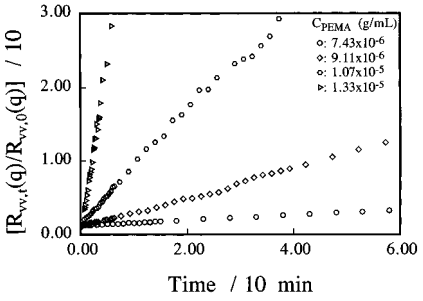

Figure 5. Time-dependence of the relative Rayleigh ratio $[R_{vv,t=t}(q)/R_{vv,t=0}(q)]$ of the STVPh9/PEMA-2 solution blend with different compositions.

It was found that the ratio of STVPh9/PEMA-2 strongly affects both the increasing rate and the final values of the apparent average hydrodynamic radius $\langle R_h\rangle$ and $R_{vv}(q)$. For the mixture with a molar ratio of STVPh9:PEMA-2 = 1:1, the precipitation occurs immediately after the mixing. The time dependence of $R_{vv}(q)$ and $\langle R_h\rangle$ can only be measured if one of the components in the STVPh9/PEMA-2 mixture is in excess. Figures 4 and 5 respectively show the time dependence of the apparent average hydrodynamic

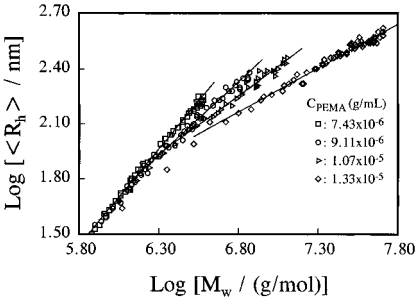

Figure 6. Double logarithmic plot of $\langle R_h \rangle$ vs M_w, where the lines represent a least-squares fitting of $\langle R_h \rangle \sim M^{\alpha}$; the exponents α are squares, 1.04; circles, 0.80; triangles, 0.63; and diamonds, 0.49.

Table 2. PEMA Concentration Dependence of the Rate of Complexation between STVPh9 and PEMA-2 in Toluene at 25 °C

C_{PEMA}-2, 10^{-5} g/mL	R_I, 1/s	R_{Rh}, nm/s
0.74	3.5×10^{-2}	7.0×10^{-1}
0.91	2.0×10^{-1}	3.0
1.07	7.9×10^{-1}	1.2×10
1.33	1.6	1.8×10

radius $\langle R_h \rangle$ and relative Rayleigh ratio of $[R_{vv,t=t}(q)/R_{vv,t=0}(q)]$, i.e., using the initial Rayleigh ratio as a reference point, where $C_{STVPh9} = 1.00 \times 10^{-4}$ g/mL and $\theta = 15°$. The linear dependence of $[R_{vv,t=t}(q)/R_{vv,t=0}(q)]$ with time indicates that the weight-average molar mass of the complexes increases at a constant rate, implying that the complexation is a diffusion-controlled process. The rate constants of $[R_{vv,t=t}(q)/R_{vv,t=0}(q)]$ and R_h estimated from the initial slope of $[R_{vv,t=t}(q)/R_{vv,t=0}(q)] \sim t$ and $\langle R_h \rangle \sim t$ are summarized in Table 2. It shows that the rate constants are greatly influenced by the PEMA-2 concentration.

Figure 6 shows the correlation of $\langle R_h \rangle$ with M_w calculated from the Rayleigh ratio on the basis of eq 1. It should be noted that M_w only represents the visible STVPh component, which is the weight-average molar mass of the STVPh chains in the complexes and individual STVPh chains. The weight fraction of PEMA in the complex is ~10% so that M_w is a good approximation of the weight-average molar mass of the complexes and individual STVPh chains. On the other hand, the scattering intensity is very sensitive to the formation of large species because $I \propto M^2$. Only a very small amount of large complexes can overshadow the scattering intensity from individual STVPh9 chains. Therefore, Figure 6 essentially represents the properties of the large complexes. Except for the very initial stages, $\log(\langle R_h \rangle)$ is a linear function of $\log(M_w)$; namely, $\langle R_h \rangle$ is scaled to M_w as $\langle R_h \rangle \sim M_w^{\alpha}$. The value of α ranges from ~1.0 to ~0.5 when C_{PEMA} increases from 7.43×10^{-6} to 1.33×10^{-5} g/mL. It is well-known that for a polymer solution, the exponent α is a constant, independent of the molar mass. The value of α is related to the polymer chain conformation; e.g., for a flexible polymer chain in a good solvent, $0.5 < \alpha < 0.6$, and for an extended polymer chain, $0.6 < \alpha \leq 1.0$. In parallel, we can also estimate the structural conformation of the complex from the value of α. Here the value of $\alpha \sim 1.0$ indicates that for a lower C_{PEMA}, the STVPh/PEMA complexes have an extended conformation, which is schematically represented by Figure 7a. The value of $\alpha \sim 0.5$ shows that for a higher C_{PEMA}, the STVPh/PEMA complexes have a "coil" conformation, as shown in Figure 7b. Figure 7 shows that as C_{PEMA} increases, the conformation of the STVPh/PEMA complexes gradually changes from an extended single-PEMA-chain complex to a multi-PEMA-chain complex. A further increase of C_{PEMA} eventually leads to the aggregation of the STVPh/PEMA complexes.

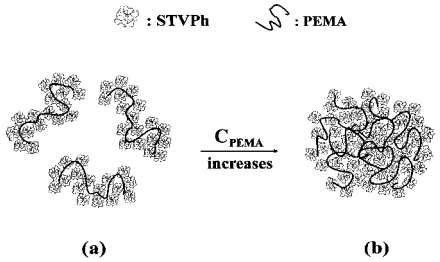

Figure 7. Schematic illustration of the structure of the STVPh/PEMA complex, where STVPh is in excess.

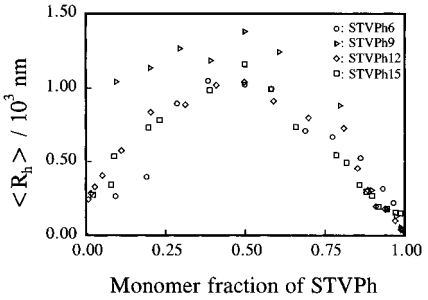

Figure 8. Composition-dependence of the average hydrodynamic radius of the STVPh/PEMA-1 complex particles with STVPh containing different phenol contents, where $\langle R_h \rangle$ is the maximum value in the plot of $\langle R_h \rangle$ vs t.

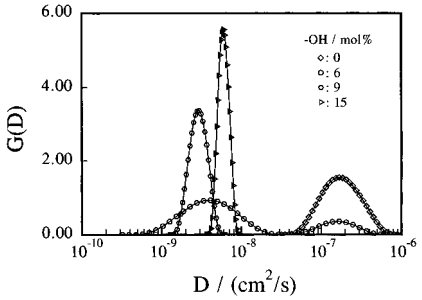

Figure 9. Comparison of the translational diffusion coefficient distributions of the STVPh/PEMA complex particles with STVPh containing different phenol contents, where the monomer ratio of STVPh/PEMA is 1:1, i.e., equimolar monomer ratio.

2. Composition Dependence of Complexation. Figure 8 shows the composition dependence of $\langle R_h \rangle$ of the STVPh/PEMA-1 complexes with different phenol contents as a function of the monomer molar fraction of STVPh, which is defined as {[styrene] + [vinylphenol]}/{[styrene] + [vinylphenol] + [ethyl methacrylate]}, where the values of $\langle R_h \rangle$ are the maximum values in the plot of $\langle R_h \rangle$ vs t, e.g., in Figure 4. It is worth noting that all curves display a maximum at the equal molar fraction; i.e., the monomer fraction of STVPh is ~ 0.5. This is consistent with the viscosity result which shows a minimum near the equimolar ratio in the viscosity−composition curves as long as the phenol content of STVPh is larger than 9 mol %.[29] The composition of the mixture with a minimum viscosity is usually regarded as the fixed mean stoichiometry (FMS) of the complexes.[30] At this composition, the solution exhibits the highest turbidity and has a maximum amount of precipitation. The hydrodynamic behavior observed in the viscosity measurements can be better revealed in dynamic LLS; namely, larger complexes can lead to

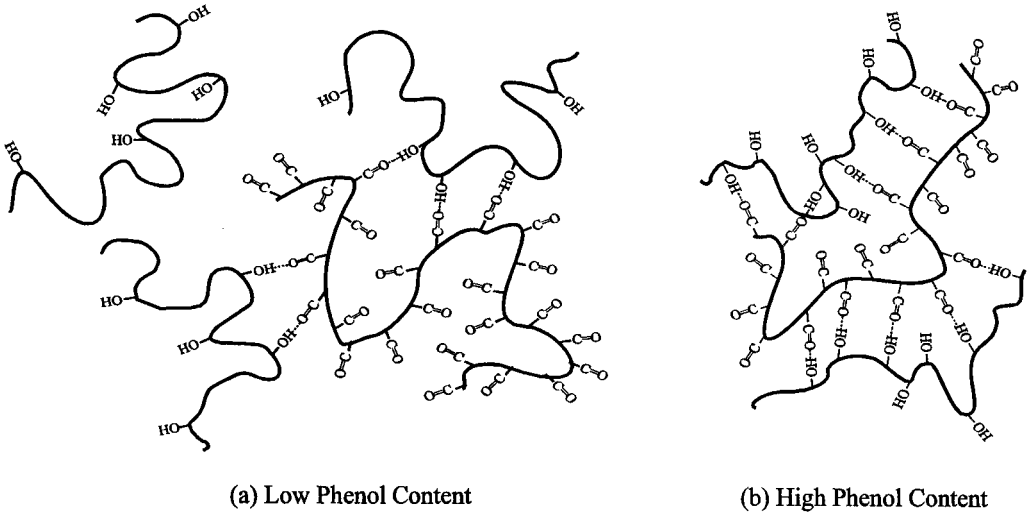

Figure 10. Schematic illustration of the complexes respectively at low and high phenol contents: (a) loose structure; (b) compact structure.

more precipitation and less individual polymer chains remain in the solution so that the solution viscosity decreases.

Figure 9 shows the phenol content dependence of the translational diffusion coefficient distribution of the STVPh/PEMA complexes, where the monomer molar ratio of STVPh/ PEMA was equal. When the phenol content is higher, the complexes show a narrow size distribution, suggesting a strong complexation between STVPh and PEMA, and the aggregation between larger and small complexes averages the initial size difference of the STVPh/PEMA complexes. Figure 10 shows a schematic diagram of the complexation respectively at low and high phenol contents.

The NRET and viscometry studies of the complexation between PS(OH) and PMMA have shown that the complexation occurs only when the hydroxyl content of PS(OH) reaches a critical value.[10] For the present system, the NRET and viscometry study showed that when the phenol content is higher than 9 mol %, the complex was observed in toluene, while in LLS, we observed that when the phenol content is higher than 6 mol %, there exists a complex as shown in Figure 8 because LLS is more sensitive to larger particles. $\langle R_h \rangle$ is only slightly dependent on the phenol content in the studied range (the phenol content is higher than 6 mol %), while $R_{vv}(q)$ is dramatically increased with the phenol content in the same phenol content range, indicating that when the phenol content is higher, more complex particles are formed or the density of the particles is higher.

3. Structure and Weight Fraction of the STVPh/PEMA Complexes. As mentioned before, the STVPh/PEMA complexes in toluene are stable for a long time if one of the components is in excess. This enables us to study the structure of the complexes using a combination of static and dynamic LLS. Figure 11 shows the composition dependence of the translational diffusion coefficient distributions of the STVPh15/PEMA-1 mixture where STVPh15 is in excess. $G(D)$ strongly depends on the amount of PEMA-1 added to the STVPh15 solution. Adding a very small amount of PEMA-1 leads to a broadening of the peak corresponding to the translational diffusion of individual STVPh15 chains. It seems that each PEMA-1 chain acts as a nucleating agent to induce complexation. Further addition of PEMA-1 leads to two distinct peaks, clearly showing the

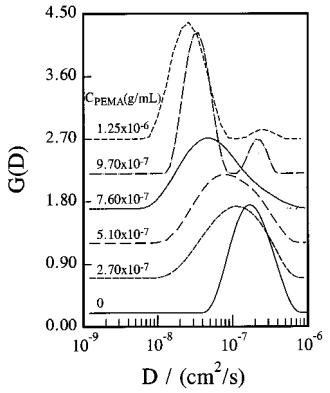

Figure 11. Typical translational diffusion coefficient distributions of the STVPh15/PEMA-1 solution blend, where STVPh15 is in excess.

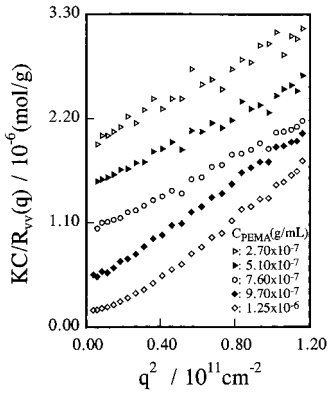

Figure 12. Angular dependence of $KC/R_{vv}(q)$ of the STVPh15/PEMA-1 solution blend with different PEMA-1 concentrations, where the total polymer concentration is 1.00×10^{-4} g/mL.

complexation between STVPh15 and PEMA-1. The hydrodynamic size of the complexes is about 10 times larger than the individual STVPh15 chains. When C_{PEMA} is 1.25×10^{-6} g/mL, the peak related to the individual STVPh15 chains nearly disappears. On average, we estimated that each PEMA-1 chain is complexed with 10−100 STVPh15 chains from dynamic LLS results.

Figure 12 shows the angular dependence of $KC/R_{vv}(q)$ of the STVPh15/PEMA-1 solutions with different amounts of PEMA-1. The curvature was expected as the amount of PEMA-1 increases, because of the forma-

Table 3. Static and Dynamic LLS Results of the STVPh15/PEMA-1 Complex Particles

$W_{STVPh15}/W_{PEMA-1}$	C_{PEMA-1}, 10^{-6} g/mL	M_w, g/mol	agg no.	$\langle R_g\rangle$, nm	$\langle R_h\rangle$, nm	$\langle R_g\rangle/\langle R_h\rangle$	x_c
pure STVPh15	0.00	3.9×10^5	1	36	26.6	1.34	0.00
363	0.27	1.54×10^7	40	96	*a*		0.06
195	0.51	1.35×10^7	35	95	*a*		0.08
158	0.63	1.35×10^7	35	98	*a*		0.11
129	0.76	1.27×10^7	33	93	*a*		0.12
100	0.97	1.44×10^7	37	103	86	1.20	0.18
80.4	1.23	1.83×10^7	48	118	136	0.86	0.28
77.4	1.25	1.25×10^7	58	127	146	0.87	0.36

[a] Two peaks are merged so that $\langle R_h\rangle$ of the complex particles cannot be determined.

tion of large complex particles. In static LLS, for a very dilute solution, the interpolymer interaction can be neglected so that the excess scattering intensity (the Rayleigh ratio) of a solution blend can be expressed as

$$R_{vv}(q\rightarrow 0) = K(M_c C_c + M_{Ph} C_{Ph}) \quad (6)$$

where K is a constant defined in eq 1, and M_c, M_{Ph}, C_c, and C_{Ph} are the molar masses and concentrations of the complexes and individual STVPh15 chains, respectively. Since STVPh15 is in excess, it is reasonable to assume that, on average, each PEMA chain is complexed with a number of STVPh15 chains. Assuming the average number of STVPh15 chains in each complex particle to be $\boldsymbol{N}$, we have

$$R_{vv}(q\rightarrow 0) = K(\boldsymbol{N} M_{Ph} C_c + M_{Ph} C_{Ph}) \quad (7)$$

where $C_c = M_c N_c$, with N_c being the molar number of complex particles and $C_{Ph} = C_T - C_c$, with C_T being the total concentration of STVPh15. If assuming each PEMA chain is surrounded by $\boldsymbol{N}$ number of STVPh15 chains in each complex particle, we have that $N_c = C_{PEMA}/M_{PEMA}$ and $M_c = \boldsymbol{N} M_{Ph}$. Equaation 7 can be rewritten as

$$R_{vv}(q\rightarrow 0) = K M_{Ph}(\boldsymbol{N}^2 N_c M_{Ph} + C_T - \boldsymbol{N} N_c M_{Ph}) \quad (8)$$

Equation 8 shows that we can calculate $\boldsymbol{N}$ from $R_{vv}(q\rightarrow 0)$ since K, M_{Ph}, N_c, and C_T are known parameters and, further, the complex's weight fraction x_c from $\boldsymbol{N}$ since $x_c = \boldsymbol{N} N_c M_{Ph}/C_T$.

Table 3 summarizes the static and dynamic LLS results, where the concentration of STVPh15 was 1.00×10^{-4} g/mL. The fact that the aggregation number ($\boldsymbol{N}$) remains essentially constant over a wide range of C_{PEMA} suggests that the complex particles have a fixed composition. The nearly constant values of $\langle R_g\rangle$ in Table 3 also support that the particles have a fixed composition which may arise from the steric effect and also the balance between the enthalpy and entropy contributions. At a low PEMA concentration, each PEMA chain is surrounded by many STVPh chains so that there is little chance for two complex particles to come together, as shown in Figure 7a. At a higher PEMA concentration, $\boldsymbol{N}$ increases as C_{PEMA} increases, indicating that two or more complex particles are interconnected by the PEMA chains.

Figure 13 shows the PEMA concentration dependence of the weight fraction of the complexes. The weight fraction is a linear function of C_{PEMA} when C_{PEMA} is low, which supports the fact that each PEMA chain is complexed with a constant number of STVPh chains. The deviation from the linear relation at a high PEMA concentration can be considered to be a result of the

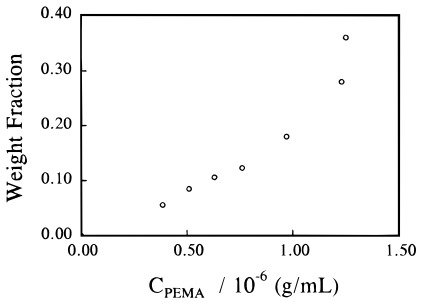

Figure 13. PEMA-1 concentration dependence of the weight fraction of the STVPh15/PEMA-1 complex particles in the solution.

multichain complexation between STVPh and PEMA. The yield of the complexation was found to exceed 30% after the addition of only 1.25 wt % PEMA into the STVPh15 solution. Moreover, the decrease of the $\langle R_g\rangle/\langle R_h\rangle$ ratio from 1.54 to 0.86 also indicates that the complex particles have spherical symmetry, shown in Figure 7b and they are more compact than individual polymer chains before the complexation.[31]

Conclusion

The laser-light-scattering results reveal the kinetics of the complexation between poly(styrene-*co*-4-vinylphenol) (STVPh) and poly(ethyl methacrylate) (PEMA) in the STVPh/PEMA solution blend. The linear dependence of $[R_{vv,t=t}(q)/R_{vv,t=0}(q)]$ with time implies that complexation is a diffusion-controlled process. The average hydrodynamic radius of the complexes can be scaled to their weight-average molar mass (M_w) as $\langle R_h\rangle \sim M_w^{\alpha}$. The value of α changes from ~1.0 to ~0.5 when the PEMA concentration increases from 7.43×10^{-6} to 1.33×10^{-5} g/mL, indicating a change of the complex conformation from an extended one to a "coiled" one. When the phenol content of STVPh is higher than 9 mol %, equimolar complexes start to form and the formation of the STVPh/PEMA complexes is controlled by the molar ratio of the monomer unit of the two polymer chains. If STVPh15 in the STVPh15/PEMA blend solution is in excess, the complex particles have a similar composition; namely, each PEMA chain acts as a nucleus and is complexed with ~35 STVPh chains. The ratio of $\langle R_g\rangle/\langle R_h\rangle$ indicates that the complex particles are compact and have spherical symmetry.

Acknowledgment. The financial support of this work by the RGC (Research Grants Council of the Hong Kong Government) Earmarked Grant 1994/95 (CUHK 453/95P, 221600460) is gratefully acknowledged. Jiang and Xiang thank the National Natural Science Foundation of China (NNSFC) for financial support.

References and Notes

(1) Jiang, M. *Chem. J. Chin. Univ.* **1991**, *12*, 127. Jiang, M. *Chem. J. Chin. Univ., Ser. B* **1990**, *B6*, 378.
(2) Smith, P.; Hara, M.; Eisenberg, A. In *Current Topics in Polymer Science*; Ottenbrite, R., Utracki, L., Inove, T., Eds.; Hanser: New York, 1987; Vol. 2, p 265.
(3) Rodriguez-PaParada, J.; Percec, V. *Macromolecules* **1986**, *19*, 55.
(4) Pearce, E.; Kwei, T. K.; Min, B. *J. Macromol. Sci., Chem.* **1984**, *A21*, 1181.
(5) Cao, X.; Jiang, M.; Yu,T. *Makromol. Chem.* **1989**, *190*, 117.
(6) Jiang, M.; Cao, X.; Chen,W.; Xiao, H.; Jin, X.; Yu, T. *Macromol. Chem., Macromol. Symp.* **1990**, *38*, 161.
(7) Jiang, M.; Chen, W.; Yu, T. *Polymer* **1991**, *32*, 989.
(8) Coleman, M. M.; Graf, J. F.; Painter, P. C. *Specific Interaction and the Miscibility of Polymer Blends*; Technomic: Lancaster, PA, 1991.

(9) Ting, S. P.; Bulkin, B. J.; Pearce, E. M.; Kwei, T. K. *J. Polym. Sci., Chem. Ed.* **1981**, *19*, 1451.
(10) Qiu, X.; Jiang, M. *Polymer* **1994**, *35*, 5084.
(11) Jiang, M.; Qiu, X.; Qin, W. *Macromolecules* **1995**, *28*, 730.
(12) Dubin, P., Bock, J., Davies, R. M., Schulz, D. N., Thies, C., Eds. *Macromolecular Complexes in Chemistry and Biology*; Springer-Verlag: Berlin, 1994.
(13) Bekturov, E. A.; Bimendina, L. A. *Advances in Polymer Science*; Springer: Berlin, Heidelberg, New York, **1981**; Vol. 41, p 99.
(14) Tsuchida, E.; Abe, K. *Advances in Polymer Science*; Springer: Berlin, Heidelberg, New York, 1982; Vol. 45.
(15) de Meftahi, M. V.; Frechet, J. M. *Polymer* **1988**, *29*, 477.
(16) Dai, J.; Goh, S. H.; Lee, S. Y.; Siow, K. S. *Polym. J.* **1994**, *26*, 905.
(17) Dai, J.; Goh, S. H.; Lee, S. Y.; Siow, K. S. *Polymer* **1994**, *35*, 2174.
(18) Wang, L. F.; Pearce, E. M.; Kwei, T. K. *J. Polym. Sci., Phys. Ed.* **1991**, *29*, 619.
(19) Xiang, M.; Jiang, M.; Feng, L. *Macromol. Rapid Commun.* **1995**, *16*, 477.
(20) Wu, C.; Xia, K.-Q. *Rev. Sci. Instrum.* **1994**, *65*, 587.
(21) Zimm, B. H. *J. Chem. Phys*, **1948**, *16*, 1099.
(22) Pizzoli, M.; Stea, G.; Ceccorulli, G.; Gechele, G. B. *Eur. Polym. J.* **1970**, *6*, 1219.
(23) Chu, B.; Wang, J.; Shuely, W. J. *Macromolecules* **1990**, *23*, 2252.
(24) Berne, B. J.; Pecora, R. *Dynamic Light Scattering*; Wiley: New York, 1976.
(25) Chu, B. *Laser Light Scattering*: *Basic Principles and Practice*; Academic: London, 1991.
(26) Provencher, S. W. *Makromol. Chem.* **1979**, *180*, 201.
(27) Stockmayer, W. H.; Schmidt, M. *Pure. Appl. Chem.* **1982**, *54*, 407.
(28) Stockmayer, W. H.; Schmidt, M. *Macromolecules* **1984**, *17*, 509.
(29) Xiang, M. Studies on Polymer-Polymer Complexation due to Hydrogen Bonding in Solution and Bulk. Ph.D. Thesis, Fudan University, Shanghai, China, **1996**.
(30) Iliopoulos, I.; Halary, J. L.; Audebert, R. *J. Polym. Sci., Polym.Chem. Ed.* **1988**, *26*, 275.
(31) Buchard, W. *Adv. Polym. Sci.* **1983**, *48*, 1.

MA961190U